
Article:
Falcini, Francesca Anna Maria, Rippin, David Manish, Krabbendam, Maarten et al. (2018) Quantifying bed roughness beneath contemporary and palaeo-ice streams. Journal of Glaciology. ISSN: 0022-1430

Quantifying bed roughness beneath contemporary and palaeo-ice streams

FRANCESCA A.M. FALCINI[1]*, DAVID M. RIPPIN[1], MAARTEN KRABBENDAM[2], KATHERINE A. SELBY[1]

[1] *Environment Department, Wentworth Way, University of York, Heslington, York, YO10 5NG*
[2] *British Geological Survey, The Lyell Centre, Research Avenue South, Edinburgh, EH14 4AP*
**Email address: famf500@york.ac.uk*

ABSTRACT. Bed roughness is an important control on ice-stream location and dynamics. The majority of previous bed roughness studies have been based on data derived from radio-echo sounding (RES) transects across Antarctica and Greenland. However, the wide spacing of RES transects means that the links between roughness and flow are poorly constrained. Here, we use Digital Terrain Model (DTM)/bathymetry data from a well-preserved palaeo-ice stream to investigate basal controls on the behaviour of contemporary ice streams. Artificial transects were set up across the Minch Palaeo-Ice Stream (NW Scotland) to mimic RES flight lines over Institute and Möller Ice Streams (Antarctica). We then explored how different data-resolution, transect orientation and spacing, and different methods, impact roughness measurements. Our results show that fast palaeo-ice flow can occur over a rough, hard bed, not just a smooth, soft bed, as previous work has suggested. Smooth areas of the bed occur over both bedrock and sediment covered regions. Similar trends in bed roughness values were found using Fast Fourier Transform analysis and standard deviation methods. Smoothing of bed roughness results can hide important details. We propose that the typical spacing of RES transects is too wide to capture different landform assemblages, and that transect orientation influences bed roughness measurements in both contemporary and palaeo-ice-stream setting.

1. INTRODUCTION

This paper aims to measure the bed roughness of contemporary subglacial and deglaciated terrains at analogous length scales. We define bed roughness as the vertical variation of terrain over a given horizontal distance (Siegert and others, 2005; Rippin and others, 2011). Accurate quantification of bed roughness beneath ice sheets is important because it is a primary control on basal drag and therefore ice flow velocity (Siegert and others, 2005; Bingham and others, 2017). Subglacial obstacles of ~0.5 to 1 m in both amplitude and horizontal wavelength have been shown theoretically to exert critical basal drag (Weertman, 1957; Kamb, 1970; Nye, 1970; Hubbard and Hubbard, 1998; Hubbard and others, 2000; Schoof, 2002); however, these obstacle dimensions lie below the resolution achievable by radio-echo sounding (RES) across ice sheets. Several authors have nevertheless explored the relationship of higher amplitude (several 100 m) and longer wavelength (100s of m to several km) bed roughness and ice dynamics across ice sheets using available RES data. These

analyses have suggested that beds beneath contemporary ice streams are relatively smooth, with roughness values decreasing downstream, whilst in surrounding areas of slower ice flow, the beds are relatively rougher (Siegert and others, 2004; Rippin and others, 2006; 2011; Callens and others, 2014). As a consequence, basal roughness is regarded as one of the controls on ice-stream location, in particular for ice streams not topographically controlled by deep valleys (Siegert and others, 2004; Bingham and Siegert, 2009; Winsborrow and others, 2010; Rippin, 2013).

While a relationship between bed roughness and ice dynamics is intuitive, quantifying such a relationship has proved elusive and several studies have produced findings that should be explored further. For example, it has been observed that fast flowing ice can also occur over a rough, hard bed (Schroeder and others, 2014). The reasons for a smooth bed underneath fast flowing ice can be varied, e.g., the existence of fine-grained sediments vs. streamlined topography (Li and others, 2010; Rippin and others, 2014). Ice-stream beds can be smooth along ice flow (parallel) and rough across flow (orthogonal) (King and others, 2009; Bingham and others, 2017), showing that the direction of bed roughness measurements is extremely important. Palaeo-ice-stream beds show the same pattern (Gudlaugsson and others, 2013; Lindbäck and Pettersson, 2015). Geology can have a strong control on the roughness underneath fast flowing ice as shown in previously glaciated gneiss terrains (Krabbendam and Bradwell, 2014). An increase in landform elongation ratios in a palaeo-ice stream has been related to the change from a rough to smooth bed (Bradwell and Stoker, 2015). The points raised by these studies demonstrate that bed roughness and its relationship to ice dynamics is complex. By using Digital Terrain Models (DTMs) from now-exposed palaeo-ice streams to calculate bed roughness, we propose that it may be possible to explore these complexities in more detail because the bed of a palaeo-ice stream can be directly observed over its entirety at much higher spatial resolutions than contemporary ice-stream beds.

The bed roughness of contemporary ice sheets has been calculated along 1D topographic profiles (from RES tracks) predominantly using two different approaches, frequency domain methods e.g. Fast Fourier Transform (FFT) analysis (e.g. Taylor and others, 2004; Siegert and others, 2005; Bingham and Siegert, 2007; Li and others, 2010; Rippin, 2013) and space domain methods e.g. Standard Deviation (SD) (Layberry and Bamber, 2001; Rippin and others, 2014). Radar specularity has also been used to infer bed roughness (e.g. Schroeder and others, 2014).The scale of bed roughness measurements has mostly been controlled by the spacing between flight tracks, and the along track resolution, which is a function of the radar system used. Ice sheet scale studies have typically used track spacing of several kilometres with an along track resolution of a few metres (Siegert and others, 2004; Rippin and others, 2006; Bingham and others, 2007). Higher resolution radar imaging by King and others (2009; 2016) and Bingham and others (2017) has shown topographic detail that cannot be captured by the larger scale studies, and is similar to the detail

available on deglaciated terrains from DTMs and bathymetric data unconstrained by ice cover (e.g. Bradwell and Stoker, 2015; Margold and others, 2015; Perkins and Brennand, 2015). Using DTMs also allows bed roughness to be measured in 2D and at much smaller scales. The resolution of DTMs is becoming finer, with pixels down to a few metres or less (e.g. LiDAR; Salcher and others, 2010; Putkinen and others, 2017). Analysis of DTMs from deglaciated areas provides an opportunity to show what is being missed when bed roughness measurements are interpolated across widely spaced RES transects. Bed roughness calculations made on this terrain can also be much more easily linked to the geomorphological and geological character of the bed, because individual landforms and geological variation can be observed directly.

In this study, we compare the bed roughness of the deglaciated, Devensian, Minch Palaeo-Ice Stream and surrounding areas in NW Scotland, with the contemporary Institute and Möller Ice Streams in West Antarctica. The bed roughness of both ice streams is quantified along transects with the same grid spacing, but for the palaeo-ice stream is also calculated between transects. We test how several parameters influence the measurement and interpretation of bed roughness. Firstly, we gauge whether the method used to measure bed roughness, FFT analysis or SD, produces different results. Secondly, we explore whether RES track spacing is sufficient to capture bed roughness trends. Thirdly, we compare bed-roughness results from transects that have the same grid spacing as RES data with results calculated down to the DTM pixel resolution. Finally, we show how the orientation of transects in relation to ice-flow direction influences bed-roughness results.

2. DATA AND METHODS

2.1 STUDY SITES AND DATA

The Minch Palaeo-Ice Stream (MPIS) drained the NW sector of the British and Irish Ice Sheet during the Devensian (Weichselian) glacial period (116 – 11.5 ka BP), and has a well-documented glacial landform and sediment record (Bradwell and others, 2008a; Bradwell and Stoker, 2015; Fig. 1). Its onset zone lies in the mountainous NW Highlands of mainland Scotland, with peaks up to c. 1000 m above present-day sea level (m a.s.l.). At its maximum extent, several ice-stream tributaries flowed from breaches (at c. 300 m a.s.l.) in the present-day watershed in the NW Highlands mainland out to the shelf edge, at c. 200 m below present-day sea level (Bradwell and others, 2007; Bradwell and Stoker, 2015; Bradwell and others, 2016; Krabbendam and others, 2016). MPIS likely reached its maximum extent at c. 26 – 28 ka (Chiverrell and Thomas, 2010; Clark and others, 2012; Praeg and others, 2015; Bradwell and others, 2016).

Institute and Möller Ice Streams (IMIS) drain the West Antarctic Ice Sheet into Ronne Ice Shelf (Fig. 1). Ice surface velocities are up to 400 m a^{-1} (Rignot and others, 2011). The inferred occurrence of sediments at the bed of Institute Ice Stream has been interpreted to be associated with a smooth bed (Bingham and Siegert, 2007; Siegert and others, 2016). The Ellsworth Trough Tributary,

111 a tributary of Institute Ice Stream, is topographically controlled (Ross and others, 2012).

112 We compare MPIS with IMIS due to their relatively comparable scale. IMIS ice thickness
113 varies between c. 50 – 3000 m (Fretwell and others, 2013). A maximum ice thickness of 750 – 1000
114 m has been modelled for MPIS (Hubbard and others, 2009; Kuchar and others, 2012). IMIS drain an
115 area of 140,000 km² and 66,000 km² respectively (Bingham and Siegert, 2009), whilst MPIS drained
116 an area of 15,000 – 20,000 km^2 (Bradwell and others, 2007; Bradwell and Stoker, 2015). Institute Ice
117 Stream is up to 82 km wide and the fast flowing section of the main trunk is 100 km long (Scambos
118 and others, 2004). MPIS was 40-50 km wide and 200 km long in total (Bradwell and Stoker, 2015).
119 MPIS had a discharge flux of 12-20 Gt a^{-1} (Bradwell and Stoker, 2015) compared to 21.6 and 6.4 Gt
120 a^{-1} for Institute and Möller Ice Streams respectively (Joughin and Bamber, 2005).

121 For contemporary ice streams in Antarctica, the data used were RES transects with an along
122 track resolution of 10 m, and a grid spacing of 30 x 10 km (Rippin and others, 2014). Data were
123 acquired in the 2010/11 austral summer using the Polarimetric Airborne Survey Instrument (PASIN)
124 with a frequency of 150 MHz (Ross and others, 2012). PASIN has retrieved bed-echoes through 4200
125 m thick ice (Vaughan and others, 2006). Crossover analysis gave RMS differences of 18.29 m for ice
126 thickness (Ross and others, 2012). The location of the data was determined using a differential GPS
127 with a horizontal accuracy of approximately 5 cm. The reflections returned from the ice-stream bed
128 were processed semi-automatically. The ice thickness (calculated every ~10 m) was subtracted from
129 ice surface elevations to calculate the bed elevations (Ross and others, 2014). For more detail on
130 acquisition and processing of the RES data see Rippin and others (2014) and Ross and others (2012;
131 2014). This dataset was used by Rippin and others (2014) to calculate bed roughness using both FFT
132 analysis and SD.

133 Figure 1 near here.

134 Two high resolution datasets were used to calculate bed roughness of the Minch Palaeo-Ice
135 Stream. For the onshore area, the NEXTMap DTM with a 5 m horizontal resolution and a 1 m vertical
136 resolution, was used (Bradwell, 2013). NEXTMap DTM tiles were downloaded from the Centre for
137 Environmental Data Analysis (CEDA) Archive (Intermap Technologies, 2009). For the offshore area,
138 Bathymetric Multi Beam Echosounder Survey data (MBES) were used. The MBES data subset has a
139 resolution of 4 m and encompasses the Little Minch and the southern area of The Minch (Fig. 1). The
140 surveys around NW Scotland were undertaken by the Maritime & Coastguard Agency (MCA)
141 between 2006 and 2012. For more detail on acquisition and processing of MBES data see Bradwell
142 and Stoker (2015) or the Reports of Survey, which can be requested from MCA, the UK
143 Hydrographic Office, the British Geological Survey or the Natural Environment Research Council.
144 MPIS is characterised by numerous elongate landforms that show a higher elongation ratio than those

in adjacent areas (Bradwell and others, 2008b). Onshore, the bed of the palaeo-ice stream is dominated by bedrock (i.e. hard-bed) landforms (Krabbendam and Bradwell, 2010; Clark and others, 2018) including bedrock megagrooves, crag and tails, whalebacks and roches moutonnées (partly within a cnoc-and-lochan landscape, especially characteristic of Scotland's northwest region, Assynt), with few soft-sediment covered landforms (e.g. Bradwell and others, 2007; Bradwell, and others, 2008b; Krabbendam and Bradwell, 2011; Bradwell, 2013). In the Minch and further offshore on the Hebrides Shelf, the bed of the palaeo-ice stream comprises more soft-sediment landforms, such as drumlinoid features, although streamlined bedrock, crag-and-tail features, and megagrooves are also present, particularly in the inner Minch (Bradwell and Stoker, 2015; Bradwell and Stoker, 2016; Ballantyne and Small, 2018). Overdeepened basins occur, in particular close to the present-day coast, which is in part characterised by a fjord system (Bradwell and Stoker, 2016; Bradwell and others, 2016). Increases in ice velocity are inferred from changes to landform elongation ratios located on the central Minch inner shelf (East Shiant Bank), which Bradwell and Stoker (2015) suggested is caused by the bed substrate changing from rough bedrock to smooth sediment.

2.2 Methods

Bed roughness along RES tracks in the Antarctic Ice Sheet and Greenland Ice Sheet has predominantly been quantified using either Fast Fourier Transform (FFT) analysis (e.g. Bingham and Siegert, 2009; Rippin, 2013; Rippin and others, 2014), or standard deviation (SD) of bed elevations (e.g. Layberry and Bamber, 2001; Rippin and others, 2014). FFT analysis transforms bed elevations into wavelength spectra (Gudlaugsson and others, 2013), producing a power spectrum (Bingham and Siegert, 2009), which is a measure of the intensity (power) of different wavelength obstacles along a transect. SD is a measure of variation in amplitude. Applied to elevation data, a higher standard deviation implies a greater spread between the high and low elevations, and thus a rougher bed. Both methods were used on MPIS and IMIS datasets to provide a comparison.

Both roughness methods were applied to a 2D dataset from a deglaciated terrain, MPIS, and were compared with a 1D dataset from a glaciated terrain, IMIS. We constructed an 'artificial' grid of transects spaced 30 x 10 km apart over the high resolution NEXTMap DTM and MBES bathymetry of the deglaciated MPIS to mimic a gridded RES survey over the glaciated IMIS (Fig. 1). The transect spacing replicates the spacing and resolution of RES transects used by Rippin and others (2014) on IMIS. Points were constructed every 10 m along all transects, and the x, y and z coordinates were extracted from NEXTMap DTM and MBES bathymetry.

Before bed roughness can be calculated using SD or FFT analysis, the elevation data have to be detrended to remove large wavelengths caused by mountains and valleys, which would otherwise dominate roughness measurements (Shepard and others, 2001; Smith, 2014). We are interested in roughness obstacles at a smaller scale than this i.e. those which affect drag. The elevation data for

each transect were detrended in R using the difference function (where difference = 2). This detrending method does not require a moving window, which removes one of many variables that affect the final bed-roughness results (Prescott, 2013; Smith, 2014). Standard deviation was then calculated along transects using a moving window size of 320 m (32 points) following previous studies (e.g. Taylor and others, 2004; Li and others, 2010). Where transects crossed lakes and coast, bed roughness values were removed to prevent bias towards smooth surfaces (Gudlaugsson and others, 2013) using the Ordnance Survey Meridian 2 lake regions shapefile (Ordnance Survey, 2017). FFT analysis requires continuous along-track data. For gaps of >100 m long (10 points), the transects were 'cut' (Rippin and others, 2014). Note that, in the onshore DTM analysis, a lake functions like a data gap. FFT analysis was not calculated across these gaps. Following previous studies (e.g. Taylor and others, 2004; Bingham and Siegert, 2009; Rippin and others, 2014), FFT analysis was calculated along transects using a window of 2^N points, where N = 5 giving a window length of 320 m (32 points). The total roughness parameter was then defined by calculating the integral of the power spectra for every window. Roughness at all scales up to the length of the window was integrated.

The bed-roughness calculations from both methods were then interpolated using the Topo to Raster tool in ArcMap, with a 1 km output cell size. The interpolated values were smoothed with a 10 km radius circle and a buffer of 2.5 km was applied either side of the transects. This allowed us to replicate the type of processed results that would be extracted from a RES survey. The same method as described above was applied to the RES transects for IMIS. The difference in bed roughness values was calculated for MPIS and IMIS at locations where transects crossed. Most SD results presented here are not normalised, but shown as absolute values in metres. However, when presented alongside the FFT results, the SD results were normalised, to enable a comparison. Following the post processing stages of interpolation, buffering, and smoothing, the data were normalised using a linear transformation. The results from both sites and both methods were re-scaled so that values range between 0 and 1.

A grid of transects spaced 2 x 2 km apart was also created for the Ullapool megagroove area (Fig. 1), a well-characterised part of the onset zone of MPIS (Bradwell and others, 2008b). This finer grid was used to measure roughness in between the gaps created when widely spaced RES grids are used underneath contemporary ice sheets. A 2 x 2 km grid allowed interpolation between transects, and was aligned approximately parallel and orthogonal to palaeo-ice flow. Roughness was calculated using the same method as the larger grid, but the interpolation resolution was 200 m, and the values were smoothed using a 2 km radius circle. Roughness was also calculated for transects parallel and orthogonal to palaeo-ice flow, allowing differences in bed roughness between palaeo-ice flow directions to be calculated. Within the area of the 2 x 2 km grid, Bradwell and others (2008b) identified a bedform continuum, which equates to an erosional transition. This transition was interpreted as a thermal boundary by Bradwell and others (2008b), and bed roughness values from the

inferred areas of warm and cold bed conditions were extracted from the smoothed interpolation, to quantify differences in roughness between these areas.

Finally, bed roughness was calculated over the entire onshore study area of the MPIS using a 2D approach. The 2D approach uses standard deviation to calculate bed roughness across surfaces, rather than along 1D transects. The 2D method allows the full coverage and resolution of the NEXTMap data to be analysed, so that bed roughness can be calculated for the gaps in between 1D transects. For every pixel, a circular window with a 320 m diameter was used for detrending and calculating bed roughness to match the results from the 1D approach. The NEXTMap DTM was detrended by subtracting a smoothed bed from the original terrain. Standard deviation was calculated from the detrended raster for each 320 m circular window. We present both unsmoothed and smoothed 2D data, to enable comparison with the smoothed 1D results. Unsmoothed 2D data allow us to look at the roughness calculations in more detail, whereas smoothed data show broader trends. Bed roughness was also calculated using the same approach above (except with a smaller 100 m window size) for all north-south pixels and all east-west pixels to assess directionality.

3. RESULTS

The 1D roughness results calculated using SD for IMIS (Fig. 2c) are, as expected, similar to those found by Rippin and others (2014) using FFT analysis (Fig. 2b). The locations of high and low values are similar but the relative magnitude of roughness trends appears reduced for SD (Fig. 2). Table 1 shows a slightly smaller range in roughness values for IMIS SD and similar means for both methods. It should be noted that SD roughness results are reported in the text as real values, but are normalised in Fig. 2 and Table 1 to enable comparison with FFT analysis. IMIS SD roughness values vary between c. 0.5 – 4 m. Lower roughness values of 0.5 – 1 m are generally located underneath the ice-stream tributaries, whereas higher roughness values (2.5 – 3.8 m) are associated with the Pirrit Hills and Nash Hills in the intertributary areas. The Ellsworth Tributary, a tributary of Institute Ice Stream, has low bed roughness values except where it joins the main trunk (~2.7 m). Similarly, Area D, a tributary of Möller Ice Stream, has mostly low roughness values, but with some higher bed roughness values (up to 2.8 m). Areas B and C, tributaries of Institute Ice Stream, generally have rougher beds than Areas A and D (up to 3.4 m). Parts of the inter-tributary area, however, have low roughness values (1 m). Thus, although there is a broad correlation between roughness and ice velocity, there are significant exceptions.

Figure 2 near here.

Table 1 near here.

The SD bed roughness values for MPIS have a lower range (0 – 1 m) compared to IMIS (0.5 – 4 m). This also applies to the normalised SD values. The FFT bed roughness values for MPIS also

have a lower range compared to IMIS (Table 1). The SD bed roughness values are lower (0.1 – 0.5 m) in the trunk of MPIS compared to the onset zones onshore (Fig. 2c). Most of the bed in the Minch is sediment covered, but some bedrock has been mapped (Fyfe and others, 1993; Bradwell and Stoker, 2015), which is slightly rougher (0.2 m) than the sediment dominated areas (0.1 m). The bedrock in the Minch is significantly smoother than the onshore bedrock of the cnoc-and-lochan landscape (Fig. 2c, d) in the onset zone (by up to 0.7 m). The 30 x 10 km grid is too low in resolution to give a detailed analysis of the transition between rough bedrock and smooth sediment in the Minch (Fig. 2). Within the Minch (bathymetry data), the flowlines coincide with smooth values (~0.1 m) (Fig. 2). This pattern contrasts with most of the flowlines in MPIS onset zones (Fig. 2), where values are rougher (0.2 – 0.9 m). This compares to higher bed roughness values from IMIS, which vary from 1 – 2.9 m and 1 – 3.8 m in the tributary and intertributary areas respectively (Fig. 2). The highest roughness values on the mainland of NW Scotland are found in the southern area (the Aird) of the 30 x 10 km grid (1 m) (Fig. 2), whilst the lowest values are concentrated in the centre and east (0.2 m) (Fig. 2). The bed roughness results from SD and FFT analysis show similar trends in high and low values for MPIS (Fig. 2c, d). For example, over the Ullapool megagrooves, both methods produce bed roughness values of 0.1 (normalised values). However, the results calculated using SD are higher overall than those calculated from FFT analysis (higher mean in Table 1). This difference is largest over the cnoc-and-lochan area, where the SD results are up to 3.5 times higher. SD bed roughness results show slightly more variation than those calculated from FFT (Fig. 2c, d). For example, bed roughness values from the top east-west transect (Fig. 2c, d) are 0.01 when calculated using FFT analysis, but vary between 0.06 and 0.1 when calculated using SD.

The bed roughness trends from the 30 x 10 km grid (Fig. 3c) match those calculated from the smoothed 2D approach (Fig. 3b) relatively well, particularly, the high roughness values over the cnoc-and-lochan landscape (3 m compared to 1 m), and low roughness values over the central and NE areas. The unsmoothed 2D results (Fig. 3a) give a much more detailed picture of bed roughness. Within the cnoc-and-lochan terrain there are significant local variations in roughness that are not apparent in the smoothed 2D data (Fig. 3a, b), whilst the bedrock of the East Shiant Bank is visible in the unsmoothed roughness data but not the smoothed (Fig. 3a, b).

Figure 3 near here.

The 2 x 2 km grid records higher roughness over the Ullapool megagrooves compared to the larger grid (0.3 m compared to 0.7 m) (Figs. 4 and 2 respectively). The distribution of bed roughness values between the areas interpreted by Bradwell and others (2008b) as cold and warm bed conditions (Fig. 4a) over the Ullapool megagrooves show a clear difference. The area with a cold bed has predominantly lower bed roughness values, with a mean of 0.2 m, compared to the area where the bed was warm, with mean of 0.4 m (Fig. 5). There is a clear transition to higher bed roughness values over

the megagrooves compared to the surrounding areas (Fig. 4a).

Figure 4 near here.

Figure 5 near here.

4. DISCUSSION

Our results show that similar patterns of bed roughness are found in both contemporary and palaeo-ice stream settings, using the same transect spacing and along-transect resolution (Fig. 2). High and low roughness values can generally be found in areas of fast ice flow. This suggests that bed roughness is not always a controlling factor on the location of ice streaming. Overall, the bed roughness results for IMIS are higher than MPIS. One reason for this difference could be the vertical resolution of RES data, which is lower compared to DTM data (5 m vs. 1 m respectively). Postglacial sedimentation could be one of the causes of this. For example, a thin layer (0.1 – 10 m) of postglacial sediment deposition occurs in the Minch (Fyfe and others, 1993; Bradwell and Stoker, 2015), which will reduce the amplitude of small scale glacial features. Yet this is unlikely to be the case onshore, where predominantly exposed bedrock with more localised areas of postglacial sediment prevails (Krabbendam and Bradwell, 2010). Conversely, topographic profiles collected using RES are an average of the radar trace (King and others, 2016), which could cause such data to be slightly smoothed in comparison to data from visible surfaces e.g. DTMs. Without being able to see the entire bed of IMIS it is difficult to provide a definitive answer. We suggest that the reason for higher bed roughness in IMIS could be due to the difference in elevation range between the two locations. MPIS has an elevation range of 1493 m, whilst IMIS has an elevation range of 3582 m (Fretwell and others, 2013).

4.1 SD vs. FFT analysis methods

Our comparison between SD and FFT analysis at the 1D scale for MPIS and IMIS showed similar broad trends of bed roughness, but there were differences (Fig. 2). For MPIS, the cnoc-and-lochan landscape appears rougher in the SD than in FFT (Fig. 2). Cnoc-and-lochan landscapes typically contain abundant lakes, which appear on a DTM as a flat surface. These are removed from the dataset to avoid bias towards a smooth surface. For FFT analysis to be carried out, transects measuring <320 m between lakes are also removed from the data, causing data gaps. Where there are multiple lakes along a transect with <320 m between them, the SD method measures a high roughness value. FFT analysis cannot capture this variation in terrain. Some transects that are not impacted by lakes also have higher bed roughness values calculated from SD compared to FFT analysis. Both methods essentially measure the amplitude of the bed obstacles (Rippin and others, 2014), but FFT analysis measures the frequency of vertical undulations (Bingham and Siegert, 2009). We suggest that the FFT

318 analysis is measuring similar frequencies of elevation change. The results from the SD method for the
319 same landscape are rougher than FFT analysis, because it is measuring large amplitude changes
320 between the numerous hills and lakes. Furthermore, FFT analysis (total roughness parameter)
321 integrates roughness at all scales up to the window size, whereas SD is calculated for the window size
322 only. This will cause higher roughness results measured using SD because the values are calculated
323 over a larger horizontal length-scale (Shepard and others, 2001). Both methods have advantages and
324 disadvantages in their application. FFT analysis emphasises roughness frequency whilst SD provides
325 a more intuitive measure of roughness scales.

326 **4.2 Transect spacing vs. complete coverage: what is missed?**

327 Measuring bed roughness on a palaeo-ice stream allows us to assess the validity of RES transect
328 spacing used to measure bed roughness on contemporary ice streams. The 30 x 10 km grid misses key
329 areas of glacial landforms used to interpret MPIS ice dynamics, such as the transition from rough
330 bedrock to smooth sediments in the bathymetry data (Fig. 2) (Bradwell and Stoker, 2015). For the
331 onshore data, shifting the 30 x 10 km grid by a few km north or south would miss the Ullapool
332 megagrooves altogether (Fig. 2). Entire inselbergs and mountain massifs are missed (blue boxes on
333 Fig. 3): in the 2D roughness maps these areas appear as very rough and it is known these had a
334 profound effect on local ice dynamics (Bradwell 2005; 2013; Finlayson and others, 2011).
335 Conversely, some areas appear rough on the 1D transect, but appear on the 2D maps as fairly smooth
336 (red boxes on Fig. 3). A much more detailed picture of 2D bed roughness trends can be achieved
337 without the smoothing employed by previous studies (Fig. 3a) (e.g. Rippin and others, 2014). For
338 example, all the cnoc-and-lochan area appears rough on the smoothed 2D data, but the unsmoothed
339 data show that some parts are smooth (Fig. 3a, b). The 2D method surpasses the detail that can be
340 captured by the 1D transects, but does not allow for analysis of the bed roughness directionality
341 (anisotropy). It is clear that exploring palaeo-ice-stream roughness is possible at much higher
342 resolutions than for contemporary ice streams, and important insights regarding the roughness of
343 subglacial terrain may thus be learnt from these environments (Gudlaugsson and others, 2013).

344 A 30 x 10 km grid is too widely spaced to capture bed roughness of some landform
345 assemblages. The question of what grid size should be used is an important one. The Ullapool
346 megagrooves for example, cover an area of 6 x 10 km, and individual grooves are up to 4 km long
347 (Krabbendam and others, 2016). A grid size of 2 x 2 km is arguably more suitable (Fig. 4). The size of
348 glacial landforms that can be measured at DTM resolution varies largely, approximately $10\text{-}10^5$ m
349 (Clark, 1993; Bennett and Glasser, 2009), and a grid size that can measure mega-groove bed
350 roughness might not be appropriate for other landform assemblages. The landscape underneath ice
351 streams has been captured in detail using RES grids with transects spaced 500 m apart (King and
352 others, 2009; King and others, 2016; Bingham and others, 2017). Importantly, these studies only used

orthogonal transects because RES can pick up multiple landform crests parallel to ice flow (King and others, 2016). Acquiring RES tracks at 500 m spacing for large areas is very challenging, but future surveys could be focused on locations where rough, streamlined topography is thought to be present (Bingham and others, 2017), or areas that could cause a future sea level rise through rapid retreat e.g. Thwaites Glacier (Joughin and others, 2014; DeConto and Pollard, 2016). Drones or Unmanned Aerial Vehicles (UAVs) have the potential to make RES data collection with small track spacing more viable over large areas (e.g. Leuschen and others, 2014).

4.3 The importance of transect orientation

The locations of high roughness values over MPIS, measured by both SD and FFT analysis along transects, do not always reflect qualitative roughness seen in the DTM and bathymetry data. This problem has been investigated previously for bed roughness (e.g. Gudlaugsson and others, 2013; Rippin and others, 2014) and englacial layers (e.g. Ng and Conway, 2004; Bingham and others, 2015), and transect orientation was shown to be important. To explore the influence of transect orientation on bed roughness we calculated bed roughness separately for north-south and east-west transects for both MPIS and IMIS (Fig. 6). Where transects cross each other, the difference in roughness was calculated (Fig. 6c, f). This was also done for transects on a pixel scale spacing for MPIS (Fig. 7). The difference in roughness of cross-cutting transects can be seen as a measure of directionality (anisotropy).

Figure 6 near here.

In MPIS some areas show a difference between east-west and north-south transects, suggesting significant anisotropy. The north-south transect along the West coast has higher roughness values (Fig. 6), notably for the lower part of the cnoc-and-lochan landscape on the exposed gneiss bedrock in the Assynt area (Krabbendam and Bradwell, 2014) and the edge of Ullapool mega grooves area (Bradwell and others, 2008b). This same pattern is also apparent in more detail at the pixel scale (Fig. 7). In the Minch the east-west pixels are rougher over the exposed bedrock (East Shiant Bank) (Fig. 7c), which is not shown in Fig. 6 because of the wide transect spacing. In both cases, the rougher transects are orthogonal to palaeo-ice flow, and support previous observations of bedrock smoothing by streaming ice (Bradwell and Stoker, 2015; Ballantyne and Small, 2018). The east-west transects crossing the Aird are rougher than the north-south transects (Fig. 6). Closer inspection of the NEXTMap DTM reveals these rough values are located where the east-west transects cross deeply incised river valleys. Post-glacial erosion or sediment deposition can impact on palaeo-ice-stream bed roughness values. In IMIS east-west transects have higher roughness values predominantly in the tributaries labelled C and D, whilst the north-south transects have higher roughness values under tributaries A and B (Fig. 6). Although the direction of these transects is not related to ice flow as analysed by Rippin and others, (2014), it shows that the direction of transects influences the bed

roughness results for both contemporary and palaeo-ice streams.

For contemporary ice streams it has been shown that the transect orientation in relation to ice flow can bias interpretation (e.g. Rippin and others, 2014; Bingham and others, 2015; Bingham and others, 2017). Parallel to ice flow, the data tend to show smooth beds (Lindbäck and Pettersson, 2015) and undisrupted ice layering (Bingham and others, 2015), whereas data orthogonal to ice flow can show rough topography (Rippin and others, 2014; Bingham and others, 2017), which can be caused by streamlined features, e.g., mega grooves or mega-scale glacial lineations (MSGLs). These landforms have strong anisotropy (Spagnolo and others, 2017). The advantage of looking at palaeo-ice-stream beds compared to contemporary ice-stream beds is that the landforms can be observed directly. The strong anisotropy of the Ullapool megagrooves, already known from traditional geomorphological studies (Bradwell and others, 2007; Krabbendam and others, 2016), is well captured by the 2 x 2 km grid results (Fig. 4b, c, d). Flow parallel transects are smoother (0.4 m), than the orthogonal transects (1 m). The roughness orthogonal to palaeo-ice flow is up to 2 x higher than parallel palaeo-ice flow. The same pattern is shown in Fig. 7. The formation of hard-bed megagrooves smooths the bed along ice-flow, but may lead to increased roughness orthogonal to ice flow, for instance by lateral plucking (Krabbendam and Bradwell, 2011; Krabbendam and others, 2016).

4.4 Roughness as a control on ice-stream location

The bed-roughness measurements extracted across MPIS using the 1D and 2D SD methods show that high roughness values occur in some areas interpreted as having hosted fast palaeo-ice flow (see MPIS flow paths, Fig. 2, 3). A rough bed underneath fast flowing ice is not typically assumed and is at odds with some previous findings from contemporary ice streams that show low roughness values i.e. a smooth bed, beneath fast flowing ice (e.g. Siegert and others, 2004; Bingham and Siegert, 2007; Rippin and others, 2011). Warm basal ice will be present in fast flowing areas whilst ice underneath slow flowing regions is likely to be frozen at the bed (Benn and Evans, 2010). Bradwell and others (2008b) interpreted areas of cold and warm basal conditions for the Ullapool megagrooves and adjacent areas (Fig. 6). Bed roughness values are lower for the areas with cold basal conditions compared to the areas with warm basal conditions (Fig. 5). Bradwell and others (2008b) identified a marked change in the bedform continuum between cold-based and warm-based zones and suggested this was due to increased ice velocity. Thus, we suggest that areas of inferred slow palaeo-ice flow can be associated with a smooth bed. Higher erosion rates under the fast flowing palaeo-ice have produced larger, elongated bedforms, which have left behind a rougher bed overall (particularly orthogonal to palaeo-ice flow). It must be noted that this is for an area of exposed bedrock, with no sediment cover.

Krabbendam (2016) argued that if there is a thick layer of temperate basal ice, fast flow can occur on a rough hard bed. In this setting, less basal drag occurs and thick temperate basal ice is

maintained by frictional heating, which produces high basal melt rates. The Laxfjord Palaeo-Ice Stream is a tributary to MPIS, identified by Bradwell (2013) (Fig. 1). Erosional landforms such as whalebacks and roches moutonnées were mapped on the bed of the Laxfjord Palaeo-Ice Stream, in the cnoc-and-lochan landscape (Bradwell, 2013). These landforms are indicative of warm based ice with meltwater present at the bed (Bennett and Glasser, 2009; Benn and Evans, 2010; Roberts and others, 2013). Bradwell (2013) suggested that topographic funnelling of ice was the driver of palaeo-fast ice flow in the Loch Laxford area. MPIS has a dendritic network of overdeepened valleys that channelled ice into a main trough, and is thought to be topographically controlled (Bradwell and Stoker, 2015). It thus appears that rough beds are possible in topographically steered ice streams, and that topographic steering may 'trump' roughness as a control on ice-stream location (see also Winsborrow and others, 2010).

Recent insights from contemporary ice streams support our results from MPIS. Schroeder and others (2014) demonstrated that the lower trunk of the fast flowing Thwaites Glacier is underlain by rough bedrock. Jordan and others (2017) found that warm-based areas, predicted by MacGregor and others (2016), underneath the northern part of the Greenland Ice Sheet, are relatively rough compared to predicted cold-based areas. A tributary to Institute Ice Stream, Ellsworth Tributary (Fig. 2), is topographically controlled (Ross and others, 2012), and Siegert and others (2016) suggest that this explains why fast flow occurs over rough areas of the bed. The suggested reasons for a rough bed underneath the Ellsworth Tributary are an absence of sediment deposition or excavation of pre-existing sediment (Siegert and others, 2016). In MPIS in Scotland and surrounding areas, there is a strong geological control on roughness (Bradwell, 2013; Krabbendam and Bradwell, 2014; Krabbendam and others, 2016). This could be the underlying cause for the rough bed underneath the Ellsworth Tributary.

Our results suggest that the bed roughness of a palaeo-ice stream and a contemporary ice stream are comparable, and support the notion that palaeo-ice streams can be used as analogues for contemporary ice streams (Bradwell and others, 2007; Rinterknecht and others, 2014; Bradwell and Stoker, 2015).

4.5 Interpreting sediment cover from roughness calculations

Bed roughness values from IMIS were smoother underneath the ice-stream tributaries compared to the intertributary areas (Fig. 2). Smooth beds beneath ice streams are typically explained by the inferred presence of soft sediment (Siegert and others, 2005; Li and others, 2010; Rippin, 2013). However, the Ullapool megagrooves (exposed bedrock features, without sediment cover) (Bradwell and others, 2008b), are smooth, particularly parallel to palaeo-ice flow (Fig. 4 and 7). Equally the East Shiant Bank includes bedrock, but is barely rougher than the adjacent, sediment-covered parts of the MPIS (Fig. 2). Smooth areas of below present-day ice streams may therefore not necessarily be

458 sediment covered.

459 **4.6 Recommendations for future studies**

460 The direction of transects influences the bed roughness results on palaeo- and contemporary ice
461 streams. We suggest that future acquisition of RES tracks over contemporary ice streams are
462 orientated parallel and orthogonal to flow where possible. Fine spacing of RES tracks i.e. 500 m
463 orthogonal to ice flow only, could be focussed on locations where the bed is thought to be rough
464 underneath fast flowing ice as this has been shown to have an impact on ice flow (Bingham and
465 others, 2017). Further analysis of the relationship between grid size, bed roughness, and landforms
466 assemblages is needed on palaeo-ice streams to give recommendations on the appropriate grid sizes.
467 For palaeo-ice streams, including MPIS, bed roughness could be explored parallel and orthogonal to
468 inferred flow lines (e.g. Gudlaugsson and others, 2013) to increase our understanding of the
469 relationship between bed roughness and ice flow direction. The bed roughness of palaeo-ice streams
470 dominated by sediment landforms (soft bed), could be compared with contemporary ice streams that
471 are thought to have similar bed properties. Palaeo-ice streams provide an opportunity to improve our
472 understanding of the relationship between landforms and bed roughness, and in turn, ice dynamics.
473 The difference in what the SD and FFT analysis methods are measuring should be taken into account
474 when these methods are applied in future studies. The effect of post-glacial erosion or sediment
475 deposition on palaeo-ice-stream bed roughness values should also be taken into consideration.

476 **5. CONCLUSION**

477 We compared the bed roughness of the deglaciated Minch Palaeo-Ice Stream (MPIS) in Scotland, to
478 the contemporary Institute and Möller Ice Streams (IMIS) in West Antarctica, using two analysis
479 methods. We also investigated whether different grid spacing and orientation impact bed roughness
480 measurements. The 30 x 10 km grid, which matches a previous RES transect distribution used for bed
481 roughness studies over a large area on contemporary ice streams, is too coarse to confidently capture
482 all the different landforms on a typical ice sheet bed. Using a finer 2 x 2 km grid we were able to
483 show that transects parallel to palaeo-ice flow were smoother compared to orthogonal transects over
484 the Ullapool megagrooves in the onset zone of MPIS. A clear difference in bed roughness values was
485 also shown for pixel scale transects for MPIS, demonstrating how transect orientation influences
486 roughness results. RES transects should be closer together in future studies and orientated in relation
487 to ice flow where possible. This would allow for more representative bed roughness measurements
488 because of the importance of flow direction on roughness patterns. SD produced similar results to
489 FFT analysis for the majority of the data, but there were some differences which should be taken into
490 account by future studies. Unsmoothed 2D roughness data for MPIS showed detail that is missed
491 when 2D data is smoothed.

492 Most MPIS flow paths in the onshore onset zones coincided with high bed roughness values,

whilst lower roughness values were associated with sediment cover in the main ice stream trunk. Yet, smooth areas of the bed beneath MPIS occurred over bedrock as well as the sediment covered areas. Low bed roughness beneath contemporary ice streams is not a reliable indicator of the presence of sediment. In this study we found that fast palaeo-ice flow has occurred over areas with high bed roughness values. Previous research often assumed that fast flowing ice streams are generally related to areas of low roughness. High and low bed roughness values were also found in the IMIS tributaries, which supports the notion that palaeo- and contemporary ice streams are comparable in terms of bed roughness. The diverse topography underneath ice streams needs to be measured in more detail to increase our understanding on what controls ice stream location. Palaeo-ice streams provide useful analogues for bed roughness underneath contemporary ice streams, and both can be used to inform the other.

ACKNOWLEDGEMENTS

This research is part of a PhD project, funded by NERC, grant number NE/K00987/1. MBES data are Crown copyright and provided by the British Geological Survey (BGS), and Maritime and Coastguard Agency. OS Meridian data are provided by the Ordnance Survey, Crown copyright and database right 2012. NEXTMap DTM was provided by NERC via the Centre for Environmental Data Analysis (CEDA). RES data came from UK NERC AFI grant NE/G013071/1. Many thanks to Jon Hill and Colin McClean from the Environment Department at the University of York, who provided advice and guidance on the methods used. We thank the editors (Hester Jiskoot and Neil Glasser) and two reviewers (Rob Bingham and one anonymous reviewer) for their helpful and insightful comments, which significantly improved this paper.

REFERENCES

Ballantyne CK and Small D (2018) The Last Scottish Ice Sheet. *Earth Env. Sci. Trans. R. Soc. Edin.* 1-39 (doi: 10.1017/S1755691018000038)

Benn DI and Evans DJA (2010) Glacier & Glaciation. Second edition. Abingdon: Hodder Education

Bennett MR and Glasser NF (2009) Glacial Geology. Second. Chichester: Wiley-Blackwell

Bingham RG and Siegert MJ (2007) Radar-derived bed roughness characterization of Institute and Möller ice streams, West Antarctica, and comparison with Siple Coast ice streams. *Geophys. Res. Lett.* **34**:1–5 (doi: 10.1029/2007GL031483)

Bingham RG, Siegert MJ, Young DA and Blankenship DD (2007) Organized flow from the South Pole to the Filchner-Ronne ice shelf: An assessment of balance velocities in interior East Antarctica using radio echo sounding data. *J. Geophys. Res*. **112**:1-11 (doi: 10.1029/2006JF000556)

526 Bingham RG and Siegert MJ (2009) Quantifying subglacial bed roughness in Antarctica: implications
527 for ice-sheet dynamics and history. *Quat. Sci. Rev.* **28**:223–236 (doi:
528 10.1016/j.quascirev.2008.10.014)

529 Bingham RG and 9 others (2015) Ice-flow structure and ice dynamic changes in the Weddell Sea
530 sector of West Antarctica from radar-imaged internal layering. *J. Geophys. Res. Earth Surf.*
531 **120**(4): 655-670 (doi: 10.1002/2014JF003291)

532 Bingham RG, Vaughan DG, King EC, Davies D, Cornford SL, Smith AM and others (2017) Diverse
533 landscapes beneath Pine Island Glacier influence ice flow. *Nat. Comms.* **8**(1618):1-9 (doi:
534 10.1038/s41467-017-01597-y)

535 Bradwell T (2005) Bedrock megagrooves in Assynt, NW Scotland. *Geomorphology*. **65**: 195-204
536 (doi: 10.1016/j.geomorph.2004.09.002)

537 Bradwell T (2013) Identifying palaeo-ice-stream tributaries on hard beds: Mapping glacial bedforms
538 and erosion zones in NW Scotland. *Geomorphology* **201**:397–414 (doi:
539 10.1016/j.geomorph.2013.07.014)

540 Bradwell T and Stoker MS (2015) Submarine sediment and landform record of a palaeo-ice stream
541 within the British − Irish Ice Sheet. *Boreas* **44**:255–276 (doi: 10.1111/bor.12111)

542 Bradwell T and Stoker MS (2016) Glacial sediment and landform record offshore NW Scotland : a
543 fjord – shelf – slope transect through a Late Quaternary mid-latitude ice-stream system. In:
544 Dowdeswell JA, Canals M, Jakobsson M, Todd BJ, Dowdeswell EK, and Hogan KA eds. Atlas
545 of Submarine Glacial Landforms: Modern, Quaternary and Ancient. London: The Geological
546 Society of London. pp. 421–428 (doi: 10.1144/M46.152)

547 Bradwell T, Stoker M, and Larter R (2007) Geomorphological signature and flow dynamics of The
548 Minch palaeo-ice stream, northwest Scotland. *J. Quat. Sci.* **22**:609–617 (doi: 10.1002/jqs.1080)

549 Bradwell T and 11 others (2008a) The northern sector of the last British Ice Sheet: Maximum extent
550 and demise. *Earth-Science Rev.* **88**:207–226 (doi: 10.1016/j.earscirev.2008.01.008)

551 Bradwell T, Stoker M and Krabbendam M (2008b) Megagrooves and streamlined bedrock in NW
552 Scotland: The role of ice streams in landscape evolution. *Geomorphology* **97**:135–156 (doi:
553 10.1016/j.geomorph.2007.02.040)

554 Bradwell T, Small D, Fabel D, Dove D, Ó Cofaigh CO and Clark C (2016) Rate and style of ice
555 stream retreat constrained by new surface-exposure ages : The Minch , NW Scotland. In: EGU.
556 Vol. 18. p. 10447

557 Callens D, Matsuoka K, Steinhage D, Smith B, Witrant E and Pattyn F (2014) Transition of flow
558 regime along a marine-terminating outlet glacier in East Antarctica. *Cryosphere* **8**:867–875 (doi:
559 10.5194/tc-8-867-2014)

560 Chiverrell RC and Thomas GSP (2010) Extent and timing of the Last Glacial Maximum (LGM) in
561 Britain and Ireland: a review. *J. Quat. Sci.* **25**:535–549 (doi: 10.1002/jqs.1404)

562 Clark CD (1993) Mega-scale glacial lineations and cross-cutting ice-flow landforms. *Earth Surf.*
563 *Process. Landf.* **18**:1-29

564 Clark CD, Hughes ALC, Greenwood SL, Jordan C and Sejrup HP (2012) Pattern and timing of retreat
565 of the last British-Irish Ice Sheet. *Quat. Sci. Rev.* **44**:112–146 (doi:
566 10.1016/j.quascirev.2010.07.019)

567 Clark CD and 13 others (2018) BRITICE Glacial Map, version 2: a map and GIS database of glacial
568 landforms of the last British-Irish Ice Sheet. *Boreas* **47**(1):11-27 (doi: 10.1111/bor.12273)

569 DeConto RM and Pollard D (2016) Contribution of Antarctica to past and future sea-level rise. *Nature*
570 **531**:591-597 (doi: 10.1038/nature17145)

571 Finlayson AG, Golledge N, Bradwell T and Fabel D (2011) Evolution of a Lateglacial mountain
572 icecap in Northern Scotland. *Boreas*. **40**(3): 536-544 (doi: 10.1111/j.1502-3885.2010.00202.x)

573 Fretwell P and 59 others (2013) Bedmap2: Improved ice bed, surface and thickness datasets for
574 Antarctica. *Cryosphere* **7**:375–393 (doi: 10.5194/tc-7-375-2013)

575 Fyfe JA, Long D and Evans D (1993) The geology of the Malin-Hebrides sea area. *United Kingdom*
576 *Offshore Reg. Rep*.

577 Gudlaugsson E, Humbert A, Winsborrow M and Andreassen K (2013) Subglacial roughness of the
578 former Barents Sea ice sheet. *J. Geophys. Res. Earth Surf.* **118**:2546–2556 (doi:
579 10.1002/2013JF002714)

580 Hubbard A and 7 others (2009) Dynamic cycles, ice streams and their imapct on the extent,
581 chronology and deglaciation of the British-Irish ice sheet. *Quat. Sci. Rev*. **28**(7-8):758-776 (doi:
582 10.1016/j.quascirev.2008.12.026)

583 Hubbard B and Hubbard A (1998) Bedrock surface roughness and the distribution of subglcailly
584 precipitated carbonate deposits: implications for the formation at Glacier de Tsanfleuron,
585 Switzerland. *Earth Surf. Process. Landforms*. **23**(3): 261-270

586 Hubbard B, Siegert MJ and McCarroll D (2000) Spectral roughness of glaciated bedrock geomorphic

surfaces: Implications for glacier sliding. *J. Geophys. Res.* **105**:21295

Intermap Technologies (2009) NEXTMap British Orthorectified Radar Image (ORI) Data by Intermap. *NERC Earth Obs. Data Cent.* [Internet]. Available from: http://catalogue.ceda.ac.uk/uuid/90de599e45a84d36a16cf01904048705

Jordan TM and 6 others (2017) Self-affine subglacial roughness: consequences for radar scattering and basal thaw discrimination in northern Greenland. *Cryosphere* **11**:1247-1264 (doi: 10.5194/tc-11-1247-2017)

Joughin I and Bamber JL (2005) Thickening of the ice stream catchments feeding the Filchner-Ronne Ice Shelf, Antarctica. *Geophys. Res. Lett*. **32**(17):1-4 (doi: 10.1029/2005GL023844)

Joughin I, Smith BE and Medley B (2014) Marine Ice Sheet Collapse Potentially Under Way for the Thwaites Glacier Basin, West Antarctica. *Science* **344**:735- 738 (doi: 10.1126/science.1249055)

Kamb B (1970) Sliding motion of glaciers: Theory and observation. *Rev. Geophys.* **8**:673–728

King EC, Hindmarsh RCA, and Stokes CR (2009) Formation of mega-scale glacial lineations observed beneath a West Antarctic ice stream. *Nat. Geosci*. **2**:585-588 (doi: 10.1038/ngeo581)

King EC, Pritchard HD and Smith AM (2016) Subglacial landforms beneath Rutford Ice Stream, Antarctica: detailed bed topography from ice-penetrating radar. *Earth Syst. Sci. Data* **8**: 151-158 (doi: 10.5194/essd-8-151-2016)

Krabbendam M (2016) Basal sliding on a rough hard bed; pressure melting and creep mechansisms in temperate basal ice. *Cryosphere* **10**:1915–1932 (doi: 10.5194/tc-10-1915-2016)

Krabbendam M and Bradwell T (2010) The geology and landscape of the Northwest Highlands: an introduction. In: Lukas S and Bradwell T (Eds.), The Quaternary of Western Sutherland and Adjacent Areas: Field Guide, Quaternary Research Association, London, 3-12

Krabbendam M and Bradwell T (2011) Lateral plucking as a mechanism for elongate erosional glacial bedforms: Explaining megagrooves in Britain and Canada. *Earth Surf. Process. Landforms* **36**:1335–1349 (doi: 10.1002/esp.2157)

Krabbendam M and Bradwell T (2014) Quaternary evolution of glaciated gneiss terrains: pre-glacial weathering vs. glacial erosion. *Quat. Sci. Rev*. **95**:20-42 (doi: 10.1016/j.quascirev.2014.03.013)

Krabbendam M, Eyles N, Putkinen N, Bradwell T and Arbelaez-Moreno L (2016) Streamlined hard beds formed by palaeo-ice streams: A review. *Sediment. Geol.* **338**:24–50 (doi: 10.1016/j.sedgeo.2015.12.007)

617 Kuchar J, Milne G, Hubbard A, Patton H, Bradley S, Shennan I and Edwards R (2012) Evaluation of
618 a numerical model of the British-Irish ice sheet using relative sea-level data: implications for the
619 interpretation of trimline observations. *J. Quat. Sci.* **27**(6): 597-605 (doi: 10.1002/jqs.2552)

620 Layberry RL and Bamber JL (2001) Between Dynamics and Basal Topography. *J. Geophys. Res.*
621 **106**:33781–33788

622 Leuschen C, Hale R, Keshmiri S, Yan JB, Rodriguez-Morales F, Mahmood A and Gogineni S (2014)
623 UAS-Based Radar Sounding of the Polar Ice Sheets. *IEEE Geosci. Remote Sens.* **2**(1):8-17 (doi:
624 10.1109/MGRS.2014.2306353)

625 Li X and 7 others (2010) Characterization of subglacial landscapes by a two-parameter roughness
626 index. *J. Glaciol.* **56**:831–836 (doi: 10.3189/002214310794457326)

627 Lindbäck K and Pettersson R (2015) Spectral roughness and glacial erosion of a land-terminating
628 section of the Greenland Ice Sheet. *Geomorphology* **238**:149–159 (doi:
629 10.1016/j.geomorph.2015.02.027)

630 MacGregor JA and 11 others (2016) A synthesis of the basal thermal state of the Greenland ice sheet.
631 *J. Geophys. Res. Earth Surf.* **121**:1328–1350 (doi: 10.1002/2015JF003803)

632 Margold M, Stokes CR and Clark CD (2015) Ice streams in the Laurentide Ice Sheet: Identification,
633 characteristics and comparison to modern ice sheets. *Earth-Science Rev.* **143**:117–146 (doi:
634 10.1016/j.earscirev.2015.01.011)

635 Mouginot J, Scheuchl B, and Rignot E (2012) Mapping of Ice Motion in Antartica Using Synthetic-
636 Aperture Radar Data. *Remote Sens.* **4**:2753-2767 (doi: 10.3390/rs4092753)

637 Ng F and Conway H (2004) Fast-flow signature in the stagnated Kamb Ice Stream, West Antarctica.
638 *Geology* **32**(6):481-484 (doi: 10.1130/G20317.1)

639 Nye JF (1970) Glacier sliding without cavitation in a linear viscour approximation. *Proc. R. Soc.*
640 *Lond. A.* **315**:381-403

641 Ordnance Survey (2017) Ordnance Survey Meridian 2. Southampton: Ordnance Survey

642 Perkins AJ and Brennand TA (2014) Refining the pattern and style of Cordilleran Ice Sheet retreat:
643 Palaeogeography, evolution and implications of lateglacial ice-dammed lake systems on the
644 southern Fraser Plateau, British Columbia, Canada. *Boreas* **44**:319–342

645 Praeg D 8 and others (2015) Ice sheet extension to the Celtic Sea shelf edge at the Last Glacial
646 Maximum. *Quat. Sci. Rev.* **111**:107–112

647 Prescott PW (2013) Quantifying subglacial roughness and its link to glacial geomorphology and ice
648 speed. Doctoral thesis, Durham University.

649 Putkinen N and 13 others (2017) High-resolution LiDAR mapping of glacial landforms and ice stream
650 lobes in Finland. *Bull. Geol. Soc. Finland.* **29**:64-81

651 Rignot E, Mouginot J and Scheuchl B (2011) Ice Flow of the Antarctic Ice Sheet. *Science* **333**:1427–
652 1430

653 Rinterknecht V and 7 others (2014) Unstable ice stream in Greenland during the Younger Dryas cold
654 event. *Geology* **42**:759–762

655 Rippin DM (2013) Bed roughness beneath the Greenland ice sheet. *J. Glaciol.* **59**:724–732

656 Rippin DM, Bamber JL, Siegert MJ, Vaughan DG and Corr HFJ (2006) Basal conditions beneath
657 enhanced-flow tributaries of Slessor Glacier, East Antarctica. *J. Glaciol.* **52**:481–490

658 Rippin DM, Vaughan DG and Corr HFJ (2011) The basal roughness of Pine Island Glacier, West
659 Antarctica. *J. Glaciol.* **57**:67–76

660 Rippin DM and 9 others (2014) Basal roughness of Institute and Möller Ice Streams, West Antarctica:
661 Process determination and landscape interpretation. *Geomorphology* **214**:139–147

662 Roberts DH, Evans DJA, Lodwick J and Cox NJ (2013) The subglacial and ice-marginal signature of
663 the North Sea Lobe of the British-Irish Ice Sheet during the Last Glacial Maximum at Upgang,
664 North Yorkshire, UK. *Proc. Geol. Assoc.* **124**:503–519

665 Ross N and 9 others (2012) Steep reverse bed slope at the grounding line of the Weddell Sea sector in
666 West Antarctica. *Nat. Geosci.* **5**:1–4

667 Ross N and 8 others (2014) The Ellsworth Subglacial Highlands: Inception and retreat of the west
668 Antarctic ice sheet. *Bull. Geol. Soc. Am.* **126**:3–15

669 Salcher BC, Hinsch R and Wagreich M (2010) High-resolution mapping of glacial landforms in the
670 North Alpine Foreland, Austria. *Geomorphology* **122**(3-4): 283-293

671 Scambos T, Bohlander J, Raup B and Haran T (2004) Glaciological characteristics of Institute Ice
672 Stream using remote sensing. *Antarct. Sci.* **16**:205–213

673 Schoof C (2002) Basal perturbations under ice streams: form drag and surface expression. *J. Glaciol.*
674 **48**(162): 407-416

675 Schroeder DM, Blankenship DD, Young DA, Witus AE and Anderson JB (2014) Airborne radar

676 sounding evidence for deformable sediments and outcropping bedrock beneath Thwaites
677 Glacier, West Antarctica. *Geophys. Res. Lett.* **41**:7200–7208

678 Shepard MK, Campbell B a, Bulmer MH, Farr TG, Gaddis LR and Plaut JJ (2001) A planetary and
679 remote sensing perspective. *J. Geophys. Res.* **106**:32,777-32,795

680 Siegert MJ, Taylor J and Payne AJ (2005) Spectral roughness of subglacial topography and
681 implications for former ice-sheet dynamics in East Antarctica. *Glob. Planet. Change* **45**:249–
682 263

683 Siegert MJ, Taylor J, Payne AJ and Hubbard B (2004) Macro-scale bed roughness of the Siple Coast
684 ice streams in west Antartica. *Earth Surf. Process. Landforms* **29**:1591–1596

685 Siegert MJ and 7 others (2016) Subglacial controls on the flow of Institute Ice Stream, West
686 Antarctica. *Ann. Glaciol.* **57**:19–24

687 Smith MW (2014) Roughness in the Earth Sciences. *Earth-Science Rev.* **136**:202–225

688 Spagnolo M and 12 others (2017) The periodic topography of ice stream beds: insights from the
689 Fourier spectra of mega-scale glacial lineations. *J. Geophys. Res. Earth Surf.* **122**:1355–1373

690 Taylor J, Siegert MJ, Payne AJ and Hubbard B (2004) Regional-scale bed roughness beneath ice
691 masses: Measurement and analysis. *Comput. Geosci.* **30**:899–908

692 Vaughan DG and 9 others (2006) New boundary conditions for the West Antarctic ice sheet:
693 Subglacial topography beneath Pine Island Glacier. *Geophys. Res. Lett.* **33**(9): 1-4

694 Weertman J (1957) On the sliding of glaciers. *J. Glaciol.* **3**:33–38

695 Winsborrow MCM, Clark CD and Stokes CR (2010) What controls the location of ice streams?
696 *Earth-Science Rev.* **103**:45–59

697

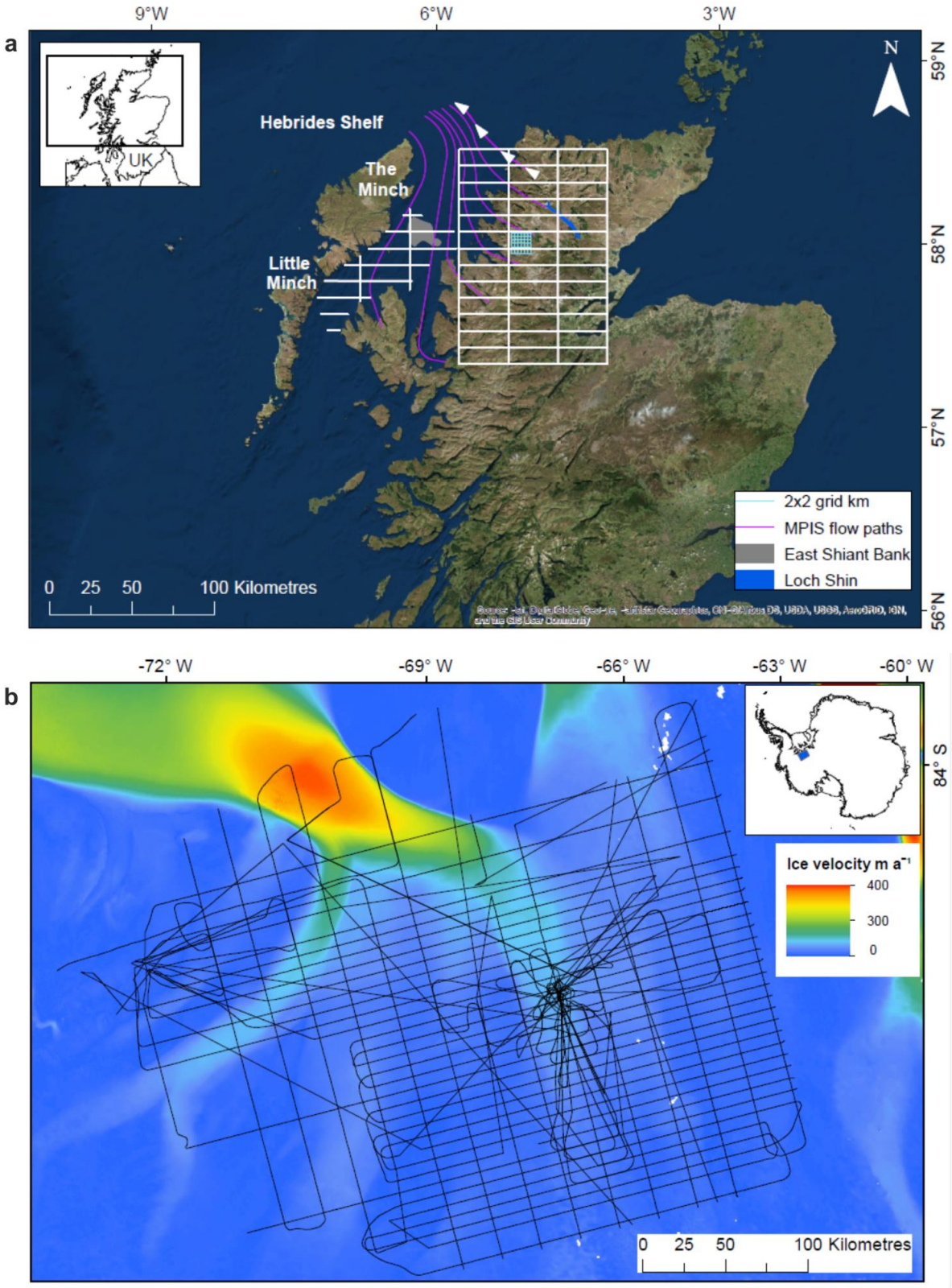

Fig. 1. Study site locations. (a) The Minch Palaeo-Ice Stream (MPIS), in NW Scotland. MPIS flow paths, i.e. areas of fast flowing ice, are from Bradwell and others (2007). The flow path with white arrows is the Laxfjord tributary. The coarse grid (30 x 10 km) set up to mimic RES transects in (b), is shown in white. The fine grid (2 x 2 km) is over the Ullapool megagroove area, and is shown in cyan. Inset map shows the location of the main image. (b) Institute and Möller Ice Streams (IMIS), in West Antarctica. RES transects are shown in black. The inset map shows the location of IMIS (blue box). Ice velocity from Rignot and others (2011) and Mouginot and others (2012).

698

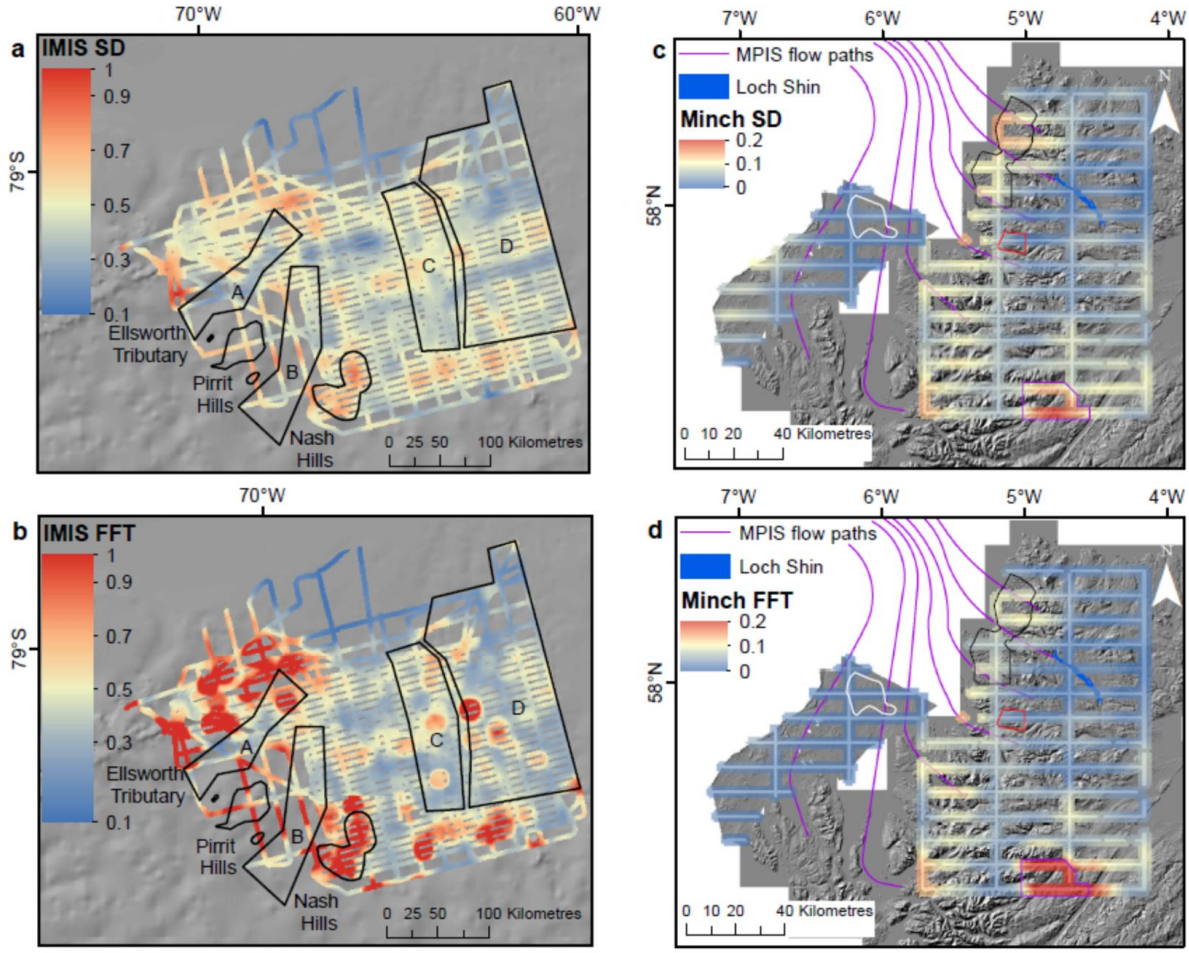

Fig. 2. Bed roughness calculated for MPIS and IMIS using SD and FFT analysis (window size = 320 m). SD and FFT data are normalised. MPIS flow paths after Bradwell and others (2007). For MPIS; the Ullapool megagrooves are outlined in red, the cnoc-and-lochan landscape (including Assynt) to the north is outlined in black, the exposed bedrock (East Shiant Bank) in the Minch is outlined in white, and the Aird is outlined in purple. For IMIS, Institute Ice Stream tributaries are labelled A, B and C, whilst the Möller Ice Stream tributary is labelled D. (a) MPIS roughness derived from SD (m). (b) MPIS roughness derived from FFT analysis (total roughness parameter). (c) IMIS roughness derived from SD (m). (d) IMIS roughness derived from FFT analysis (total roughness parameter).

699

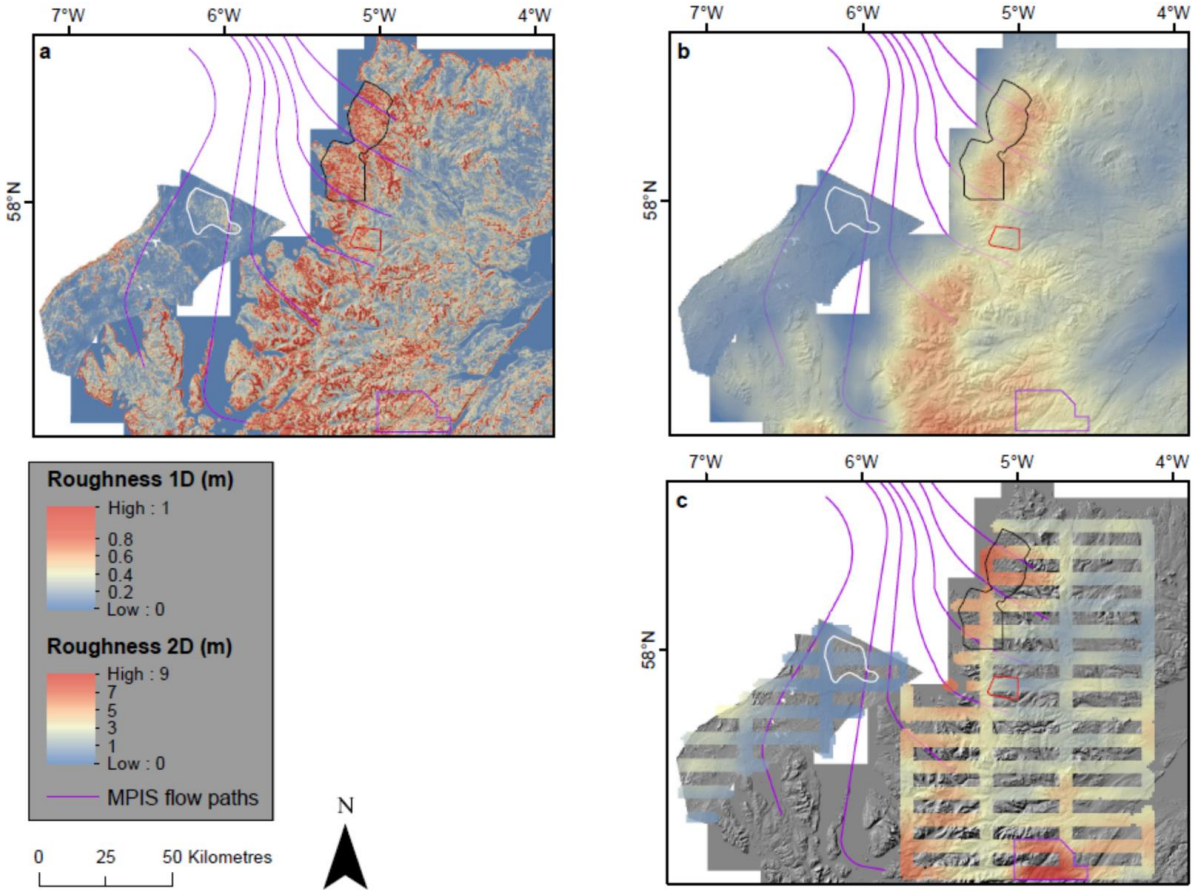

Fig. 3. Bed roughness calculated using SD for all NEXTMap DTM pixels using a moving window of 320 m (2D). Values are not normalised. The exposed bedrock (East Shiant Bank) in the Minch is outlined in white. The Ullapool megagrooves are outlined in red. The cnoc-and-lochan landscape (including the Assynt) to the north is outlined in black. The Aird is outlined in purple. (a) Bed roughness of MPIS onset zone with flow paths after Bradwell and others (2007). Blue boxes are inselbergs and mountain massifs that are missed by the 1D 30 x 10 km transects. These include: Ben Mor Coigach massif, Ben Stack, the Assynt massif, the Fannichs, and Liathach. Red boxes show Loch Ewe and Little Loch Broom, which appear rough on the 1D grid but smooth using the 2D data. (b) Bed roughness from (a) that has been resampled to 1 km resolution and smoothed using the same window size as that used for the bed roughness measurements calculated using the 30 x 10 km grid. (c) Bed roughness from the 1D 30 x 10 km.

700

701

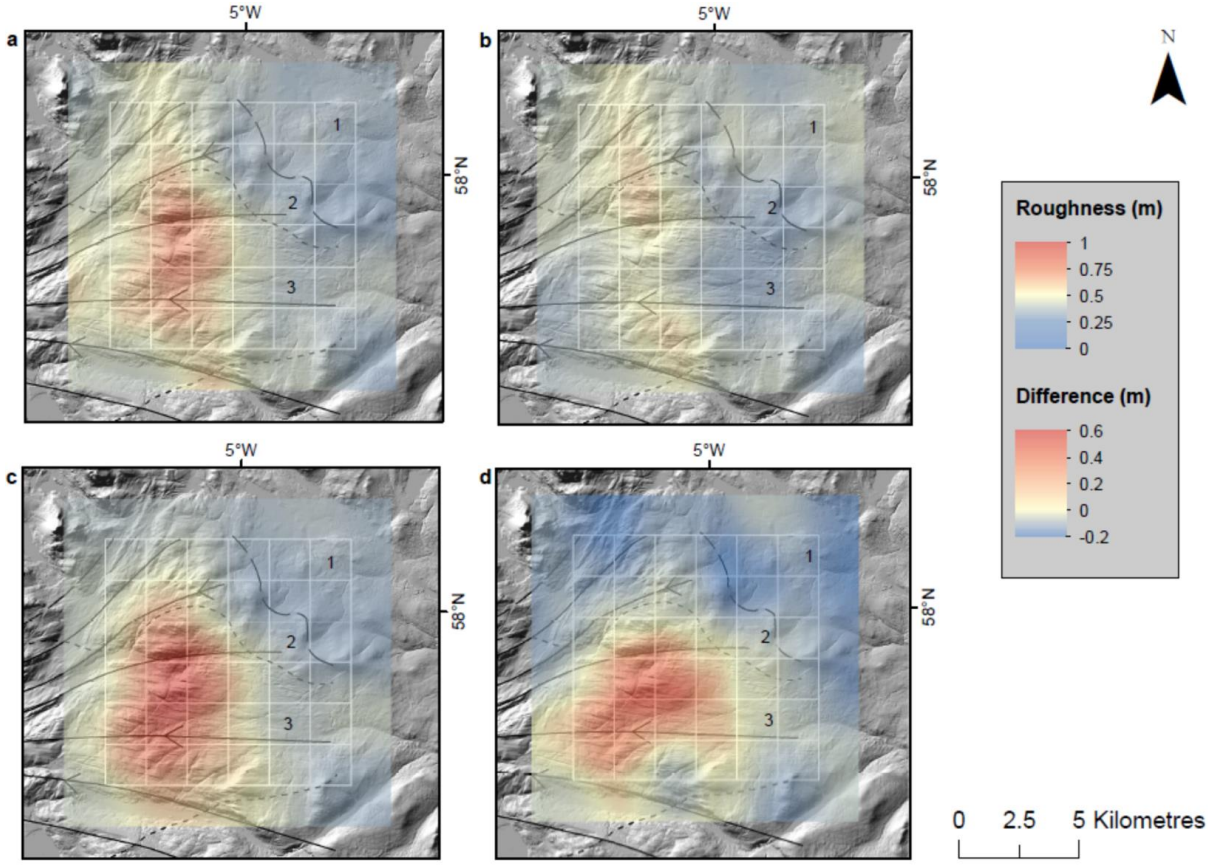

Fig. 4. Roughness measured along transects (white lines, grid spacing of 2 x 2 km) over the Ullapool megagrooves (see Fig. 1 for location). The transects are approximately parallel and orthogonal to palaeo-ice flow (Solid black lines with arrows, east to west). 1 is an area of no glacial streaming (cold based ice), 2 is an area of subtle streamlined landforms between the dotted and dashed lines (warm based ice). Between the dotted lines, 3 is an area of strong glacial streamlining (warm based ice). Palaeo-flow direction and areas of glacial streaming after Bradwell and others (2008b). Values are not normalised. (a) Roughness calculated along all transects. (b) Roughness calculated along transects parallel to flow. (c) Roughness calculated along transects orthogonal to flow. (d) The magnitude difference between (b) and (c).

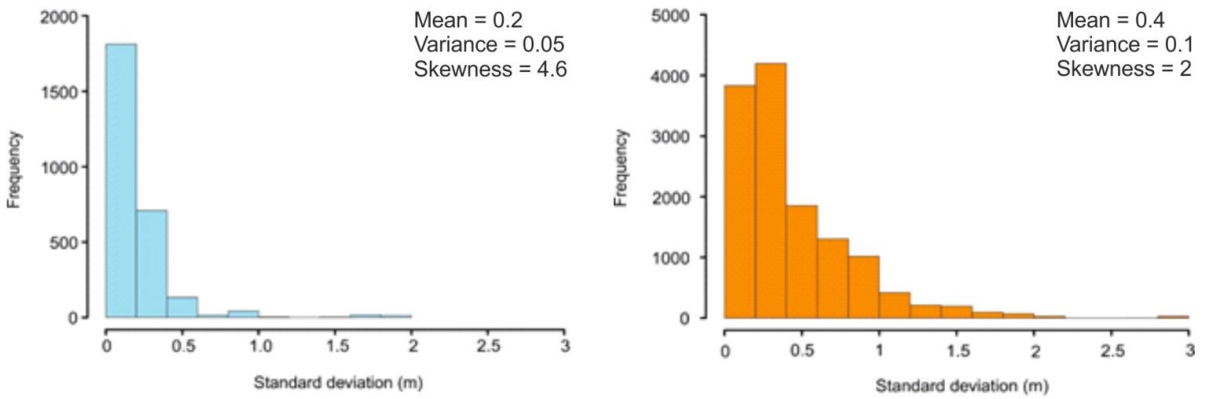

Fig. 5. Bed roughness distributions in cold-based (blue) and warm-based (orange) areas from the 2x2 km grid over the Ullapool megagrooves. Cold-based and warm-based areas are defined by Bradwell and others (2008b). Values are not normalised.

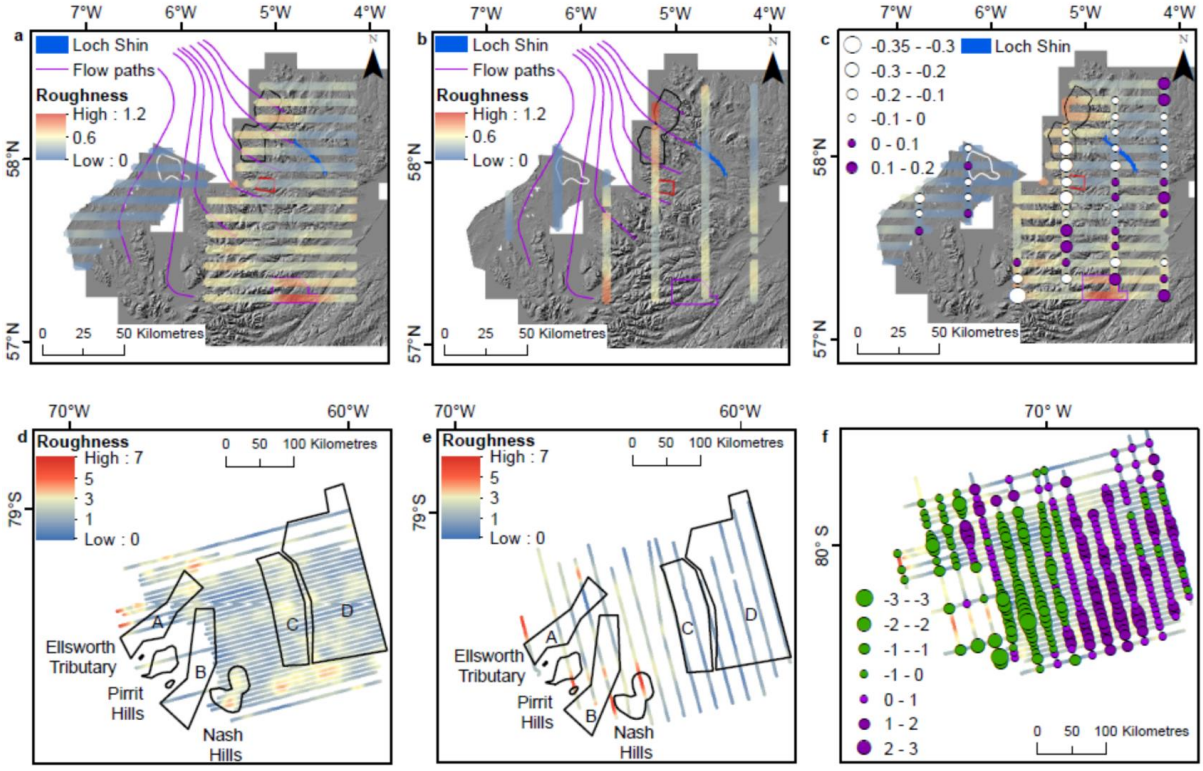

Fig. 6. The relationship between bed roughness measurements and transect orientation for MPIS and IMIS. All bed roughness measurements were calculated using SD and values are not normalised. For MPIS: The exposed bedrock (East Shiant Bank) in the Minch is outlined in white. The Ullapool megagrooves are outlined in red. The cnoc-and-lochan landscape (including the Assynt) to the north is outlined in black. The Aird is outlined in purple. (a) Bed roughness for east-west MPIS transects. (b) Bed roughness for north-south MPIS transects. (c) The proportional circles show the east-west transects minus the north-south for MPIS. (d) Bed roughness for east-west IMIS transects. (e) Bed roughness for north-south IMIS transects. (f) The proportional circles show the east-west transects minus the north-south transects for IMIS.

707

708

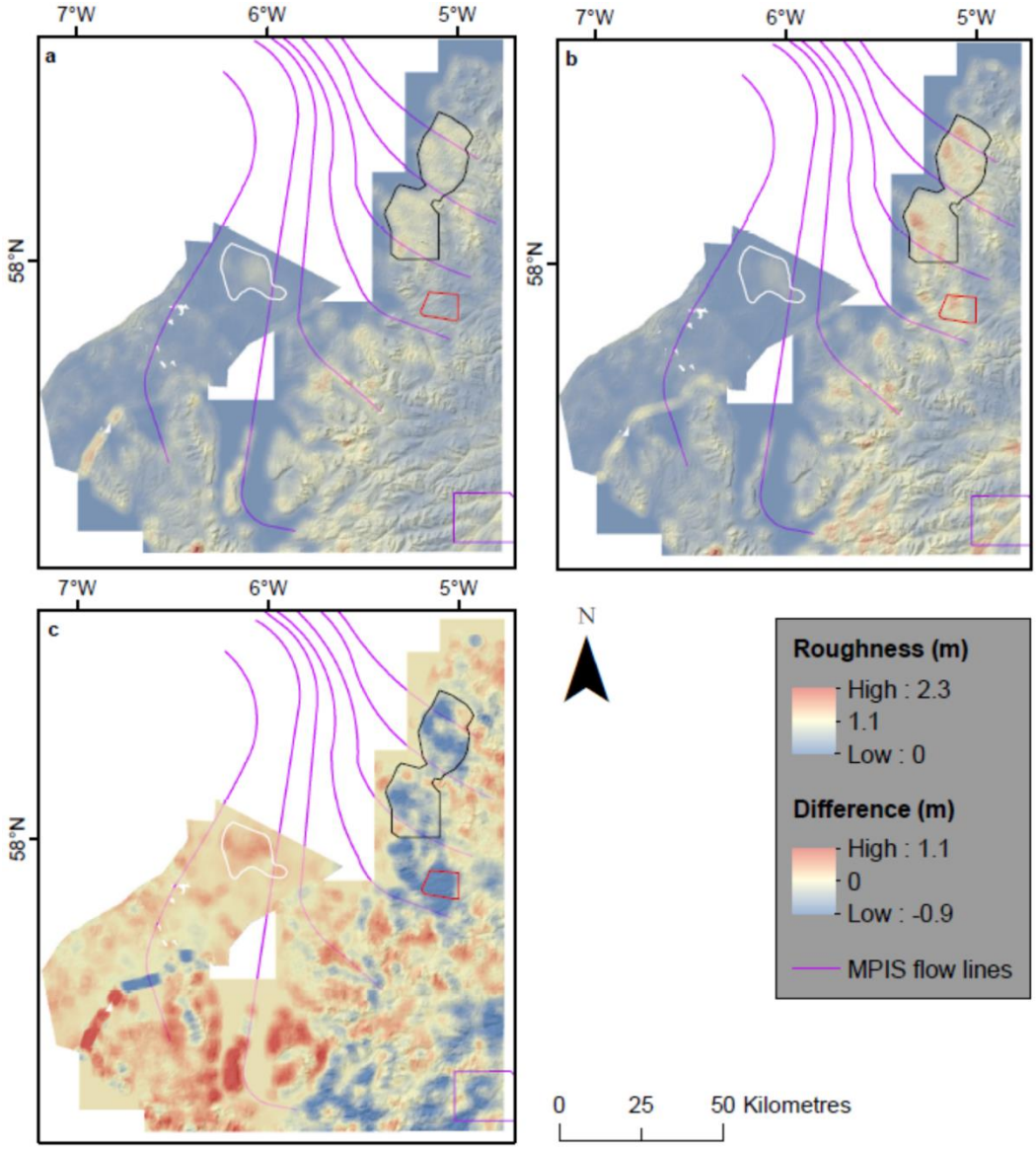

Fig. 7. The relationship between bed roughness measurements and transect direction for MPIS on a pixel scale. All bed roughness measurements were calculated using SD (window size = 100 m) and values are not normalised. The same interpolation and smoothing done for Fig. 4 was used here. The exposed bedrock (East Shiant Bank) in the Minch is outlined in white. The Ullapool megagrooves are outlined in red. The cnoc-and-lochan landscape (including Assynt) to the north is outlined in black. The Aird is outlined in purple. (a) Bed roughness values calculated for each row of the DTM (east-west). (b) Bed roughness values calculated for each column of the DTM (north-south). (c) Plot of east-west minus north-south bed roughness.

715 **Table 1.** Statistics of bed roughness results for MPIS and IMIS, using both methods. These are normalised
716 values. The maximum value and minimum value across all data sets was used to normalise.

Site location and roughness method	Range	Minimum	Maximum	Mean
MPIS SD	0.25	0	0.25	0.08
MPIS FFT analysis	0.25	0	0.25	0.03
IMIS SD	0.9	0.1	1	0.46
IMIS FFT analysis	1	0	1	0.49

717

718